RESEARCH ARTICLE

Influence of low-temperature combustion and dimethyl ether-diesel blends on performance, combustion, and emission characteristics of common rail diesel engine: a CFD study

Venkatesh Tavareppa Lamani[1] · Ajay Kumar Yadav[1] · Kumar Gottekere Narayanappa[1]

Abstract Due to presence of more oxygen, absence of carbon-carbon (C-C) bond in chemical structure, and high cetane number of dimethyl ether (DME), pollution from DME operated engine is less compared to diesel engine. Hence, the DME can be a promising alternative fuel for diesel engine. The present study emphasizes the effect of various exhaust gas recirculation (EGR) rates (0–20%) and DME/Diesel blends (0–20%) on combustion characteristics and exhaust emissions of common rail direct injection (CRDI) engine using three-dimensional computational fluid dynamics (CFD) simulation. Extended coherent flame model-3 zone (*ECFM-3Z*) is implemented to carry out combustion analysis, and *k-ξ-f* model is employed for turbulence modeling. Results show that in-cylinder pressure marginally decreases with employing EGR compared to without EGR case. As EGR rate increases, nitrogen oxide (NO) formation decreases, whereas soot increases marginally. Due to better combustion characteristics of DME, indicated thermal efficiency (ITE) increases with the increases in DME/diesel blend ratio. Adverse effect of EGR on efficiency for blends is less compared to neat diesel, because the anoxygenated region created due to EGR is compensated by extra oxygen present in DME. The trade-off among NO, soot, carbon monoxide (CO) formation, and efficiency is studied by normalizing the parameters. Optimum operating condition is found at 10% EGR rate and 20% DME/ diesel blend. The maximum indicated thermal efficiency was observed for DME/diesel ratio of 20% in the present range of study. Obtained results are validated with published experimental data and found good agreement.

Abbreviations

A,b	Arrhenius equation coefficients
BDC	Bottom Dead center
BTDC	Before Top Dead center
C_s	Soot
D_t	Diffusion coefficient
$\widetilde{E}_{\widetilde{F} \to M}$	Activation energy
$\widetilde{E}_{\widetilde{F}u,M}$	Unmixed fuel
$\widetilde{E}_{O_2}$	Unmixed oxygen
E_{act}	Activation energy
ECFM3Z	Extended coherent flame model three zone
EVC	Exhaust valve close
EVO	Exhaust valve open
IMAP	Intake manifold pressure
IMAT	Intake manifold temperature
IVC	Inlet valve close
IVO	Inlet valve open
M_{Fuel}	Molar mass of fuel
M^{Mol}	Mean molar mass of the gases in the mixed area
NO	Nitrogen oxide
R	Universal gas constant
$\overline{S}_{NO}$	Mean nitric oxide source
S_c and S_{ct}	Laminar and turbulent Schmidt numbers
TDC	Top Dead center
$\tilde{u}$	Density-weighted average velocity

Responsible editor: Philippe Garrigues

✉ Ajay Kumar Yadav
ajaykyadav@nitk.edu.in

[1] Department of Mechanical Engineering, National Institute of Technology Karnataka, Surathkal, Mangalore 575 025, India

Greek letters

ζ	Transformed coordinate system
$\overline{\rho}^u$	Density
μ	Dynamic viscosity
ε	Dissipation rate
ϕ	Equivalence ratio
τ_d	Ignition delay
$\overline{\omega}_x$	Average combustion source term

Introduction

Energy crisis, rise in fuel costs in the world market and growing consciousness about environment pollution related to petroleum fuels, created global interest in alternative fuels. Alternative fuel should have minimum tail pipe emission and renewable features. Dimethyl ether (DME) is recognized as an environment friendly alternative fuel for multiple markets, such as power generation, domestic home cooking, transportation, and as a chemical intermediate (Semelsberger et al. 2006). Due to presence of more oxygen and absence of C-C bond in chemical structure of dimethyl ether, pollution from DME operated engine is less compared to diesel engine (Verbeek et al. 1996). DME has high cetane number, and similar fuel properties to diesel; hence, it is a suitable alternative to diesel (Arcoumanis et al. 2008). It has been observed that DME engine in integration with exhaust gas recirculation (EGR) meets the stringent emission regulations (Ying and Longbao 2008). Lee et al. (2011) examined the combustion, performance, and emission characteristics of diesel engine operated with *n*-butane and DME blend. Result shows that even for neat DME fuel, stable engine operations were observed under wide range of loads. Power output and fuel consumptions were improved with blend. Zhu et al. (2012) found that DME engine operated under different injection timings emits lesser total hydro carbon (THC), less NOx, and smoke-free combustion. Wang et al. (2013) conducted experiments on effect of DME energy ratio on DME-diesel dual fuel premixed charge compression ignition (PCCI) engine. Smoke emission for PCCI engine decreases with increase in DME ratio. They also reported that NOx emission reduces initially and increases marginally as DME/diesel ratio increases. The NOx emission for DME engine is higher than diesel engine, but with increase in engine speed, it tends to reduce (Cipolat 2007).

Due to its good self-ignition and highly volatile characteristics, DME yields almost smoke-free combustion (Teng et al. 2004; Sorenson 2001). Diesel engine operated with oxygenated fuel was found to be decreased in volatile organic compound at medium load (Rezgui and Guemini 2014). To reduce exhaust emissions such as carbon monoxide and hydrocarbon, oxidation catalyst is required in diesel engine (Kapus and Cartellieri 1995). Though burning velocity of DME is similar to petrol, it is not suitable for SI engine due to its higher cetane number (Daly et al. 2001). Compared to natural gas, DME was found to be superior for gas turbine fuel (Basu and Wainwright 2001). DME spray has smaller sauter mean diameter compared to diesel which helps in fast evaporation of fuel droplets (Kajitani et al. (2000) and Yao et al. (2003)). Kim et al. (2008) investigated injection behavior of DME and its effect on exhaust emission characteristics of CI engine. They observed the escalation in nitrogen oxides and significantly decrease in CO and HC emission due to faster evaporation and oxygen content in the fuel. Park and Lee (2013) conducted numerical study on DME fuelled CI engine, and they observed that DME is easy to handle same as LPG, because it condenses to liquid state at 0.5 MPa pressure and atmospheric temperature. DME can be produced from varieties of feed stock; hence, it is a suitable alternative fuel for diesel engine. Bo et al. (2006) investigated the effect of introducing DME in single cylinder four-stroke diesel engine with slight modification. DME was heated to 1000 K, and emulsified diesel was used as a fuel; they observed that BSFC gets reduced by 10%. Huang et al. (2009) conducted experimental studies on performance, combustion, and emission characteristics of DME-operated CI engines. DME-operated engine were maintained at higher injection rate and fuel quantity in order to maintain the same power as that of diesel engine. At low- and medium-engine speeds, the brake-specific fuel consumption (BSFC) of DME is better than that of diesel fuel. However, at high engine speed, the fuel consumption will increase due to the lower heating value of DME.

DME gets evaporated at atmospheric condition; hence, it has to be stored in a cylinder in compressed form (more than 0.3 MPa) so that liquid DME can be directly supplied to high-pressure fuel injection pump (Suh and Lee 2008). Announcement of Bio-DME as a diesel fuel in commercial vehicle by Volvo created a global interest. Various international and national associations like International DME Association (IDA), Korea DME Forum (KDF), China DME Association (CDA), and Japan DME Forum (JDF) are established to do imminent research on DME as alternative fuel.

Detailed CFD studies on combustion and emission characteristics of direct injection engines using DME/diesel blends are very scant in open literature. In this study, we explore the details of variations in the engine performance, tailpipe emissions, and combustion characteristics for various DME/diesel blends and EGR rates. The CFD simulation is carried out for a four-stroke CRDI engine to better comprehend the in-cylinder combustion. Such study is not available in open literature.

Engine details

CRDI engine used by Mobasheri et al. (2012) and Han et al. (1996) is considered for CFD simulation in the present work. The details of the engine and injection system are listed in Table 1.

Fuel properties

The key properties of diesel and DME fuels are listed in the Table 2 (Arcoumanis et al. 2008).

Computational model

CFD code and meshing of geometry

AVL ESE CFD tool is used for Engine Geometric modeling and meshing as portrayed in Fig. 1a. Complete 3-D CFD simulation is carried out using the AVL platform (AVL Fire version 2011). The injector with six holes is situated centrally on the top of piston; hence, 60° sector is selected as computational domain. In order to reduce the computational time, high-pressure cycle is considered in the present work. Simulation is started and ended at inlet valve close and exhaust valve open position, respectively. Grid independence test has been carried out to obtain optimum grid size as shown in Fig. 1b, c. Simulation is carried out on 64 GB RAM 32 core work station with

parallel processing. Results have been checked for peak pressure, peak temperature, and computational time for various grid sizes. It is found that the considered output parameters are invariant with change in total number of grids at/after 4×10^5. Boundary conditions and models employed in the simulation are listed in Tables 3 and 4, respectively.

Governing equations

The transport equations for chemical species modeled as

$$\frac{\partial\left(\overline{\rho}\tilde{Y}_x\right)}{\partial t} + \frac{\partial\left(\overline{u}_i\overline{\rho}\tilde{Y}_x\right)}{\partial x_i} = \frac{\partial}{\partial x_i}\left(\left(\frac{\mu}{S_c} + \frac{\mu}{S_{ct}}\right)\frac{\partial\tilde{Y}_x}{\partial x_i}\right) + \overline{\omega}_x \quad (1)$$

The fuel transport equations are (Colin and Benkenida 2004)

$$\frac{\partial\left(\overline{\rho}\tilde{Y}_{Fu}^u\right)}{\partial t} + \frac{\partial\left(\overline{\rho}\tilde{u}_i\tilde{Y}_{Fu}^u\right)}{\partial x_i} = \frac{\partial}{\partial x_i}\left(\left(\frac{\mu}{S_c} + \frac{\mu_t}{S_{ct}}\right)\frac{\partial\tilde{Y}_{Fu}^u}{\partial x_i}\right) \quad (2)$$
$$+ \overline{\rho}\tilde{S}_{Fu}^u + \overline{\omega}_{Fu}^u - \overline{\omega}_{Fu}^{u \to b}$$

$$\frac{\partial\left(\overline{\rho}\tilde{Y}_{Fu}^b\right)}{\partial t} + \frac{\partial\left(\overline{\rho}\tilde{u}_i\tilde{Y}_{Fu}^b\right)}{\partial x_i} = \frac{\partial}{\partial x_i}\left(\left(\frac{\mu}{S_c} + \frac{\mu_t}{S_{ct}}\right)\frac{\partial\tilde{Y}_{Fu}^b}{\partial x_i}\right) \quad (3)$$
$$+ \overline{\rho}\tilde{S}_{Fu}^b + \overline{\omega}_{Fu}^b - \overline{\omega}_{Fu}^{u \to b}$$

The equations for these unmixed species are

$$\frac{\partial\left(\overline{\rho}\tilde{Y}_{Fu}^F\right)}{\partial t} + \frac{\partial\left(\overline{\rho}\tilde{u}_i\tilde{Y}_{Fu}^F\right)}{\partial x_i} - \frac{\partial}{\partial x_i}\left(\left(\frac{\mu}{S_c} + \frac{\mu_t}{S_{ct}}\right)\frac{\partial\tilde{Y}_{Fu}^F}{\partial x_i}\right) = \overline{\rho}\tilde{S}_{Fu}^F + \overline{\rho}\tilde{E}_{Fu}^{F \to M}$$
$$(4)$$

$$\frac{\partial\left(\overline{\rho}\tilde{Y}_{O_2}^A\right)}{\partial t} + \frac{\partial\left(\overline{\rho}\tilde{u}_i\tilde{Y}_{O_2}^A\right)}{\partial x_i} - \frac{\partial}{\partial x_i}\left(\left(\frac{\mu}{S_c} + \frac{\mu_t}{S_{ct}}\right)\frac{\partial\tilde{Y}_{O_2}^A}{\partial x_i}\right) = \overline{\rho}\tilde{E}_{O_2}^{A \to M} \quad (5)$$

Table 1 Engine specifications

Engine parameters	Values
Bore × stroke	0.13719 m × 0.1651 m
Compression ratio	15.1:1
Connecting rod length	0.26162 m
Displacement	2441 cm³
IVO/IVC	32° BTDC/147° BTDC
EVO/EVC	134° ATDC/29° ATDC
Engine speed	1600 RPM
IMAP	184,000 N/m²
IMAT	310 K
Injector parameters	Values
Injector type	Common rail
Injection pressure	90 MPa
Number of nozzle holes	6
Nozzle hole diameter	0.00026 m
Injection duration	21.5° CA
Start of injection	9° BTDC
Fuel injected	0.0001622 kg/cycle

From Mobasheri et al. (2012) and Han et al. (1996)

Table 2 Properties of blending stocks

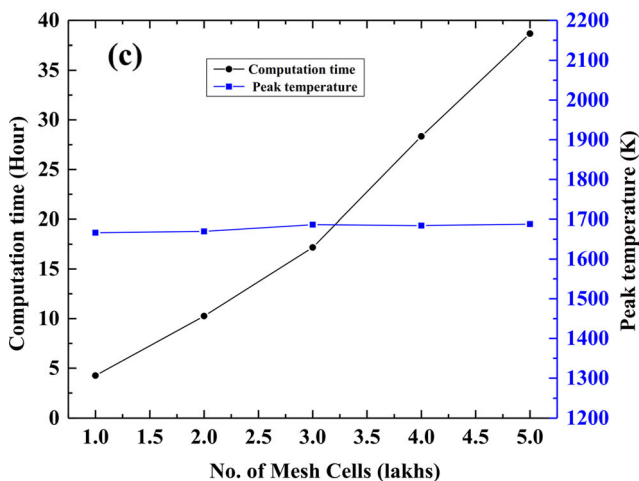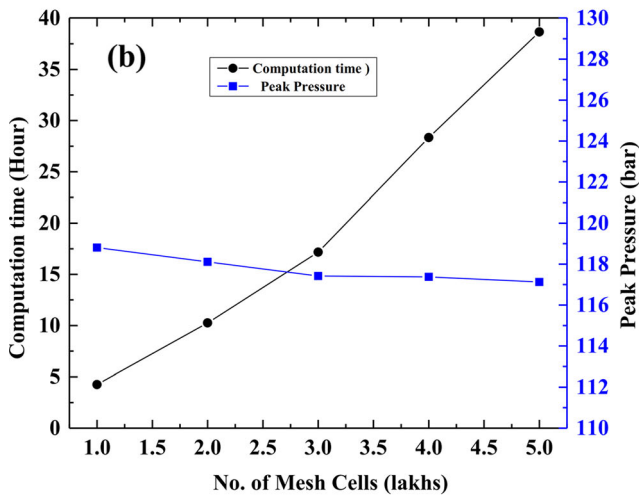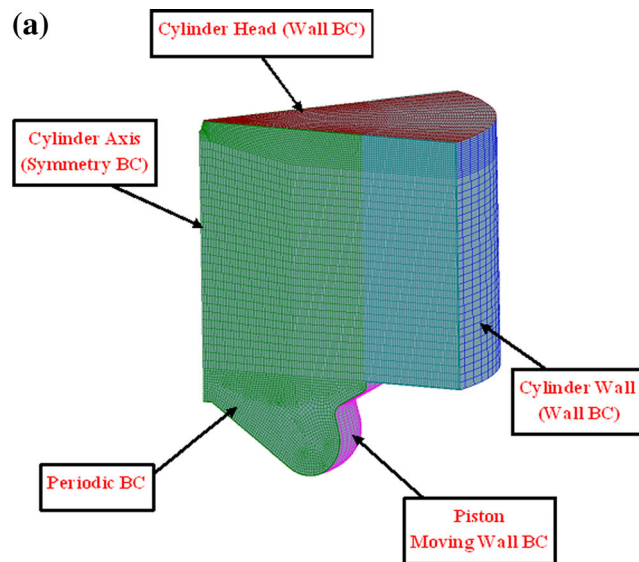| Properties	Diesel	DME
Boiling point (°C)	180–330	−23
Density, g/ml at 20 °C	0.84	0.606
Oxygenate (wt%)	–	34.8
Hydrogen (wt%)	13	13
Viscosity, cS at 40 °C	3.11	0.12–0.15
Cetane number	46	55–66
Gross heat content (MJ/kg)	42.5	27.6

(a)

(b)

(c)

Fig. 1 **a** Three-dimensional computational domain at TDC position. **b** Grid independence study carried out for peak pressure. **c** Grid independence study carried out for peak temperature

The amount of mixing is computed with a characteristic time scale based on the k-ε model.

$$\overline{E}_{Fu}^{F\to M} = -\frac{1}{\tau_m}\tilde{Y}_{Fu}^{F}\left(1-\tilde{Y}_{Fu}^{F}\frac{\overline{\rho}M^M}{\frac{u}{\rho}\big|_u M^u_{Fu}}\right) \quad (6)$$

$$\overline{E}_{O_2}^{A\to M} = -\frac{1}{\tau_m}\tilde{Y}_{O_2}^{A}\left(1-\frac{\tilde{Y}_{O_2}^{A}}{\tilde{Y}_{O_2}^{\infty}}\frac{\overline{\rho}M^M}{\frac{u}{\rho}\big|_u M^u_{air+EGR}}\right) \quad (7)$$

where τ_m is the mixing time defined as

$$\tau_m^{-1} = \frac{\varepsilon}{k} \quad (8)$$

The oxygen mass fraction in unmixed air is computed as follows:

$$\tilde{Y}_{O_2}^{\infty} = \frac{\tilde{Y}_{TO_2}}{1-\tilde{Y}_{TFu}} \quad (9)$$

Pollutant model

The transport equation model for Nitrogen monoxide is given by

$$\frac{\partial\left(\overline{\rho}\tilde{Y}_{NO}\right)}{\partial t}+\frac{\partial\left(\overline{u}_i\overline{\rho}\tilde{Y}_{NO}\right)}{\partial x_i}=\frac{\partial}{\partial x_i}\left(\overline{\rho}D_t\frac{\partial\tilde{Y}_{NO}}{\partial x_i}\right)+\overline{S}_{NO} \quad (10)$$

The term $\overline{S}_{NO}$ represents source term for NO_x formation in the equation.

$$\overline{S}_{NO} = M_{NO}\left(\frac{dc_{NO\ thermal}}{dt}+\frac{dc_{NO\ prompt}}{dt}\right) \quad (11)$$

The transport equation model for formation mass fraction ϕ_s is given by

$$\frac{\partial}{\partial t}\left(\overline{\rho}\tilde{\phi}_s\right)+\frac{\partial}{\partial x_j}\left(\overline{\rho u_j}\overline{\phi}_s\right)=\frac{\partial}{\partial x_j}\left(\frac{\mu_{eff}}{\sigma_s}\frac{\partial\overline{\phi}_s}{\partial x_j}\right)+S_{\varphi_s} \quad (12)$$

Soot formation rate is defined as

$$S_{\varphi_s} = S_n + S_g + S_{o_2} \quad (13)$$

where S_n = soot nucleation, S_g = soot growth, and S_{o_2} = soot oxidation.

Table 3 Calculation domain and boundary conditions

Boundary type	Boundary condition	Values
Piston	Moving mesh	Temperature 550 K
Axis	Periodic inlet/outlet	Periodic
Cylinder head	Wall	Temperature 550 K
Compensation volume	Wall	Thermal/adiabatic boundary
Liner	Wall	Temperature 425 K

EGR

The EGR rate in steady-state operation can be defined as the ratio of EGR mass flow rate ($\dot{m}_{egr}$) and the total intake mass flow rate ($\dot{m}_{intake}$).

$$\dot{m}_{intake} = \dot{m}_{air} + \dot{m}_{egr} \qquad (14)$$

$$EGR = \dot{m}_{egr}/\dot{m}_{intake} \qquad (15)$$

Validation

In the present study, the engine simulation software AVL-FIRE is coupled with CHEMKIN II with detailed reaction mechanisms. The simulation is validated from the literature (Mobasheri et al. 2012; Han et al. 1996) for conditions listed in Table 1. Equivalence ratio obtained for diesel engine in the present study is 0.47. Results are obtained for in-cylinder pressure and heat release rate versus crank angle portrayed in Fig. 2. Simulation results show a good agreement with published experimental data.
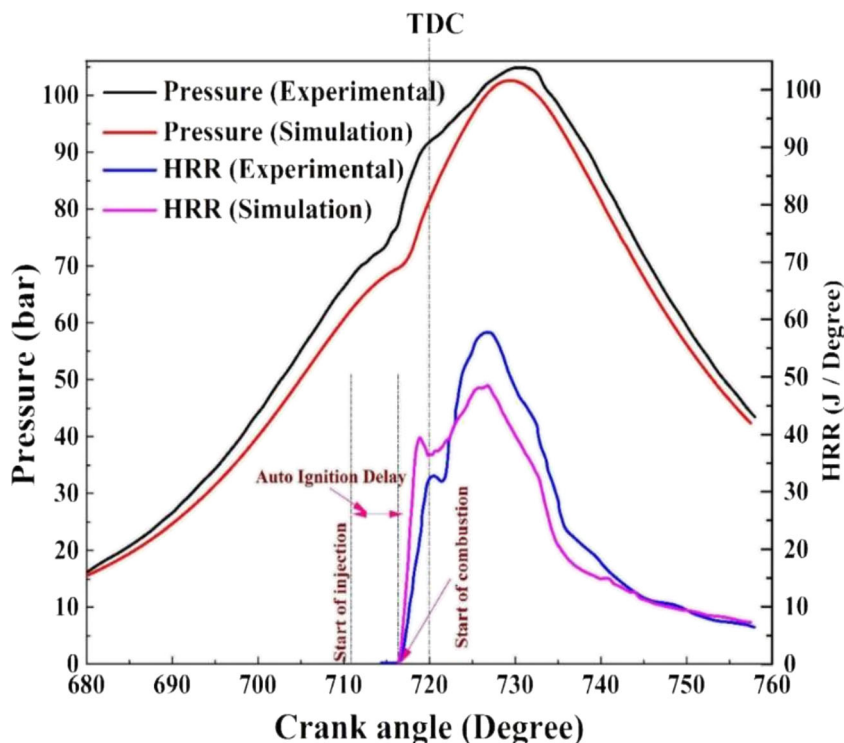
Results and discussion

Results are obtained for various DME/diesel blends ratio (0, 5, 10, 15, 20%) various EGR rates (0, 5, 10, 15, 20%) in the three-dimensional CFD simulation. Amount of the fuel injected is kept constant (0.0001622 kg/cycle) in all the cases.

Effect of various DME/diesel blends and EGR rates on engine performance

The effect of low temperature combustion and DME/diesel blend ratio on performance of CRDI engine is demonstrated in Fig. 3. The higher cetane number, more oxygen content, active evaporation, and low viscosity improve combustion characteristics for DME/diesel operations compared to the neat diesel (DME0). Simulation is run for various DME/diesel blends (0–20%) and different EGR rates (0–20%). Results show the increase of ITE with DME/diesel blends and found to be highest in the case of DME20 EGR (5–10%). The adverse effect of EGR rate on ITE is insignificant in the case of DME/diesel, and it is significant in neat diesel operations. Hence, for lower NOx emission, higher EGR can be applied in the case of blends unlike neat diesel (Table 5).

Table 4 Models employed in CFD simulation

Model	Options
Turbulence model	*k-ζ-f Model*
Breakup model	Wave
Turbulent dispersion model	Enable
Wall treatment	Hybrid wall treatment
Wall impingement model	Walljet 1
Heat transfer wall model	Standard wall function
Evaporation model	Dukowicz and multi-component model
Combustion model	CFM
Ignition model	ECFM-3Z
Soot formation and oxidation	Kinetic Model
NO_x mechanism	Extended Zeldovich
Chemistry solver	Fire internal chemistry interpreter (CHEMKIN-II)

Fig. 2 In-cylinder pressure versus crank angle for validation with experimental results

Effect of various DME/diesel blends and EGR rate on in-cylinder pressure

Figure 4a, b shows the effect of the DME/diesel blends and EGR rates on in-cylinder pressure, respectively. As DME diesel blends ratio increases, the in-cylinder peak pressure increases as shown in the Fig. 4a. It occurs due to decrease in ignition delay with addition of DME. For all the cases, ignition delay increases with increase in EGR rates due to reduction in oxygen availability and increase in specific heat capacity of mixture, as exhaust gas contains species of higher specific heat capacity. Hence, if EGR rate increases, cylinder pressure decreases as the result of combustion delay.

Effect of various DME/diesel blends and EGR rate on in-cylinder temperature

Figure 5a, b shows the effect of EGR and various DME blends on in-cylinder temperature, respectively. The cylinder temperature is one of the core features for controlling the auto-ignition process. EGR decreases the oxygen concentration in combustion chamber and circulates the gases like H_2O and CO_2 of very high-specific heat capacity. This composition acts like a thermal sink and reduces the adiabatic flame temperature of the cylinder. As EGR rate varies from 0 to 20%, the peak value of in-cylinder mean temperature decreases. In-cylinder temperature is found higher for higher DME/diesel blend ratio due to better combustion in DME/diesel blends case as explained above in Fig. 3.
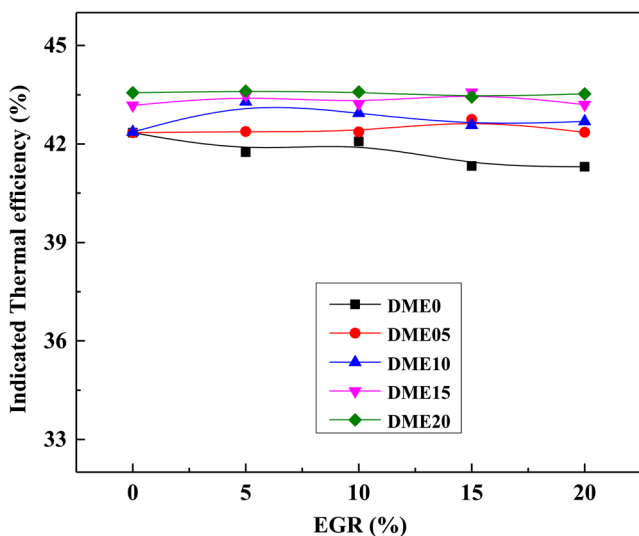

Fig. 3 Effects of DME/diesel blends ratio and EGR rate on ITE

Table 5 Torque for various EGR and DME-Diesel blends

Torque (N/m)					
EGR (%)	0	5	10	15	20
DME00	228.30	225.06	226.87	219.57	222.67
DME05	224.06	224.25	224.16	226.22	224.1
DME10	219.95	224.72	222.90	218.95	221.59
DME15	219.79	221.41	220.05	221.87	219.94
DME20	217.41	217.66	217.53	216.75	217.27

Fig. 4 a Effects of EGR rate on in-cylinder pressure. b Effects of DME/diesel blends ratio on in-cylinder pressure
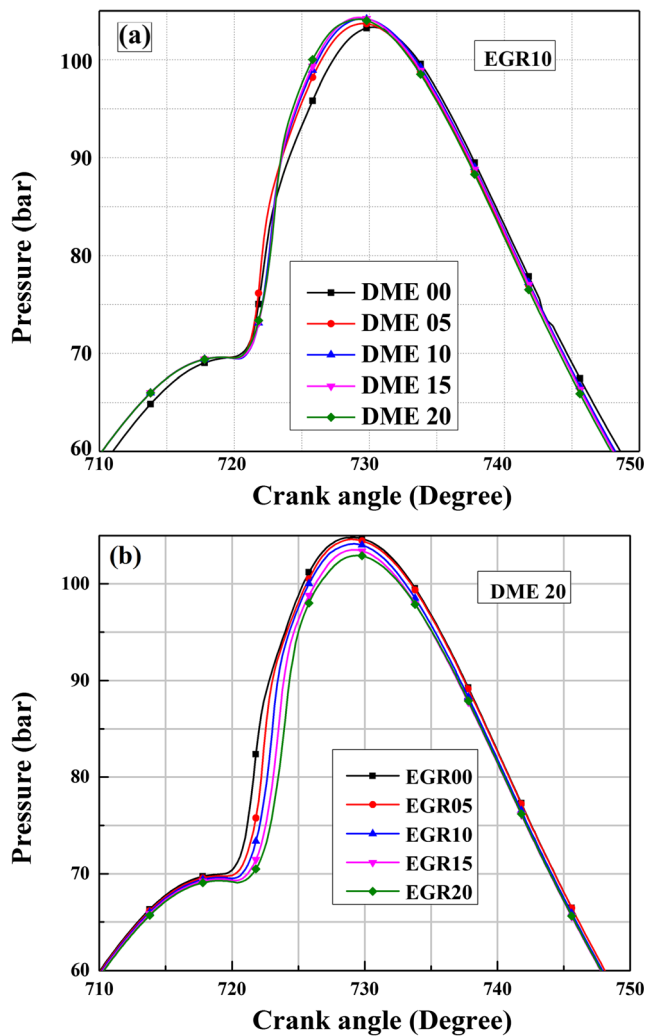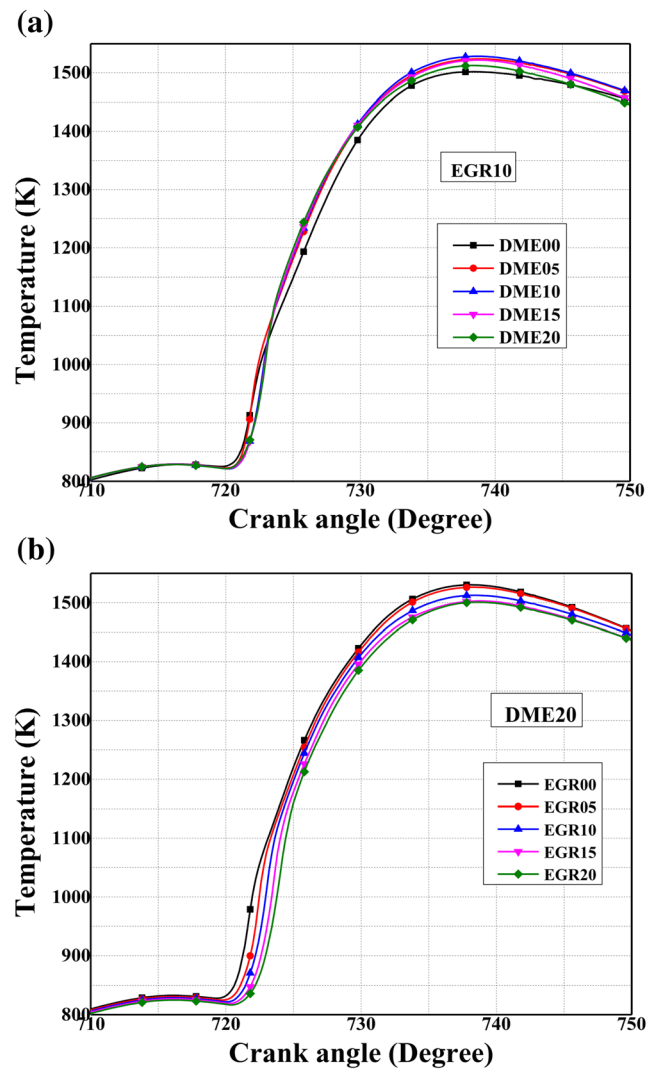

Fig. 5 a Effects of EGR rate on in-cylinder temperature. b Effects of DME/diesel blends ratio on in-cylinder temperature

Effect of various DME/diesel blends and EGR rate on in-cylinder CO formation

Figure 6 shows the illustration of the CO formation for various DME/diesel blends at different EGR rates. CO formation trend is similar for all cases; the CO formation decreases with increase in DME/diesel blends and increases with EGR rates. Less CO formation is observed for DME20 blend with 5% EGR rate and found to be decreased by 48% compared to neat diesel without EGR. It occurs due to extra oxygen present in DME which causes oxidation of CO.

Effect of various DME/diesel blends and EGR rate on NO formation

The in-cylinder NO formation is explained by majorly Zeldovich mechanism, prompt, and fuel-bound nitrogen (Fattah et al. 2014). The key parameters to nitrogen oxide formation are local temperature, residence time, and

concentration of oxygen in higher flame temperature zone. Figure 7 shows the well-established advantage of EGR in decreasing NOx emissions from diesel engine. For all DME/diesel blends (0–20%) and EGR rates (0–20%), NO formation is marginally higher than neat diesel due to higher in-cylinder temperature as explained in Fig. 5b. Similar trend is also observed by Kim et al. (2008). More cetane number and fuel-bounded oxygen of DME compared to diesel results in higher NO formation. Less NO formation is observed for EGR20 for all DME/diesel blends compared to without EGR case. It has been noticed that there is a significant drop in NO formation approximately by 60% (overall) due to EGR.

Effect of various DME/diesel blends and EGR rate on soot formation

Figure 8 shows the effect of DME/diesel blend and EGR rate on soot formation. The DME-fuelled engine exhausts very
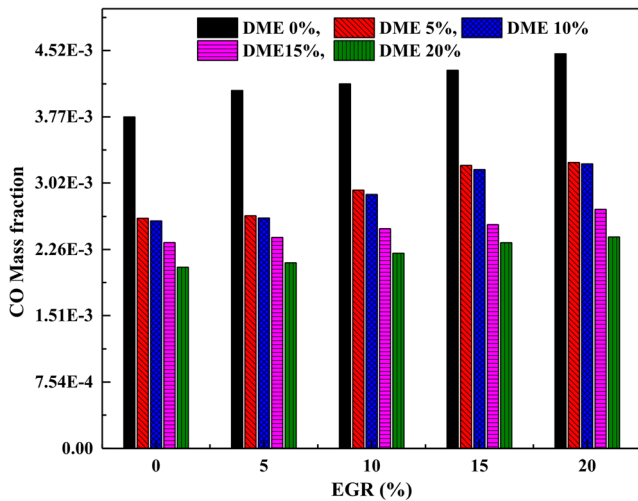
Fig. 6 Effects of DME/diesel blends ratio and EGR rate on CO mass fraction

Fig. 7 Effects of DME/diesel blends ratio and EGR rate on NO mass fraction

less soot emissions due to its chemical compositions. Formation of soot occurs in rich fuel and medium temperature zone. The precursors of soot, i.e., acetylene and polycyclic aromatic hydrocarbons (PAH), play a key role in soot formation (Jeon et al. 2014). The formation of the precursors depends largely on radicals with carbon-carbon bonds in the fuel chemical structure (Ying and Longbao 2008). The chemical structure for DME (CH_3-O-CH_3) fuel contains no C-C bonds and has more oxygen content which causes high particulate oxidation and suppresses soot formation. EGR decreases the oxygen concentration inside the combustion chamber which leads to a partial combustion and the high soot formation. It has been observed that with more EGR rate, in-cylinder soot formation increases. Results are compared for DME0 without EGR rate with various blends (DME5, DME10, DME15, and DME20) and different EGR rates (5, 10, 15, and 20%). Less soot formation is observed for DME20 blend (25%) compared to DME0 for without EGR case.

As EGR increases, the effect of blends on PM is not significant. In the present range of study, it is noticed that the effect of blends (10, 15, and 20%) on reduction in soot formation at 20% EGR is almost constant. Soot formation takes place due to the combined effect of in-cylinder temperature as well as oxygen content in the charge. Increase in oxygen content enhances the soot oxidation, whereas decrease in temperature increases the soot formation. In-cylinder temperature decreases due to increase in blend and EGR rates (Fig. 6a, b), whereas oxygen contents increase with blends and decreases with EGR. Finally, the overall effect of these parameters on soot formation is marginal at higher blend and EGR rates.

Improved exhaust emissions trade-off

Figure 9a, b illustrates the normalized emissions (NO, soot, and CO) versus EGR rates and DME/diesel blends, respectively.
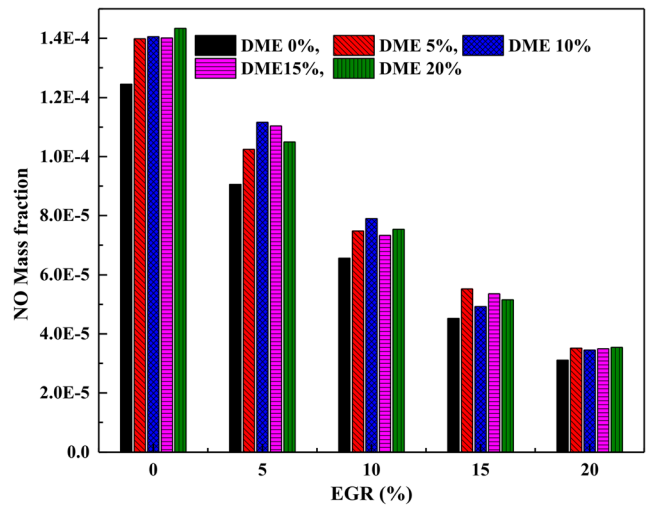
Normalized emission values for all the cases are obtained with respect to the diesel fuel. By comparing the considered parameters, a trade-off can be established to optimize the operating conditions near to 10% EGR. Based on emission norms, higher EGR (20%) can be considered with minor loss of efficiency to get lower value of NOx. As discussed above, maximum efficiency is obtained at DME20 in present range of study. Figure 9b shows that the CO and soot emissions are minimum with marginal increases in NO for DME20. From the present study, it can be concluded that DME20 with EGR20 yields optimum performance with less emissions.

Conclusions

In the present study, CFD simulation is carried out to determine the effects of DME/diesel blend ratio and EGR rates on the
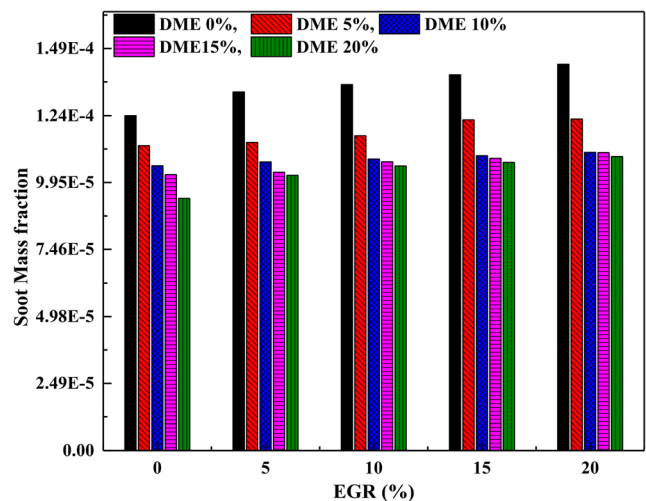

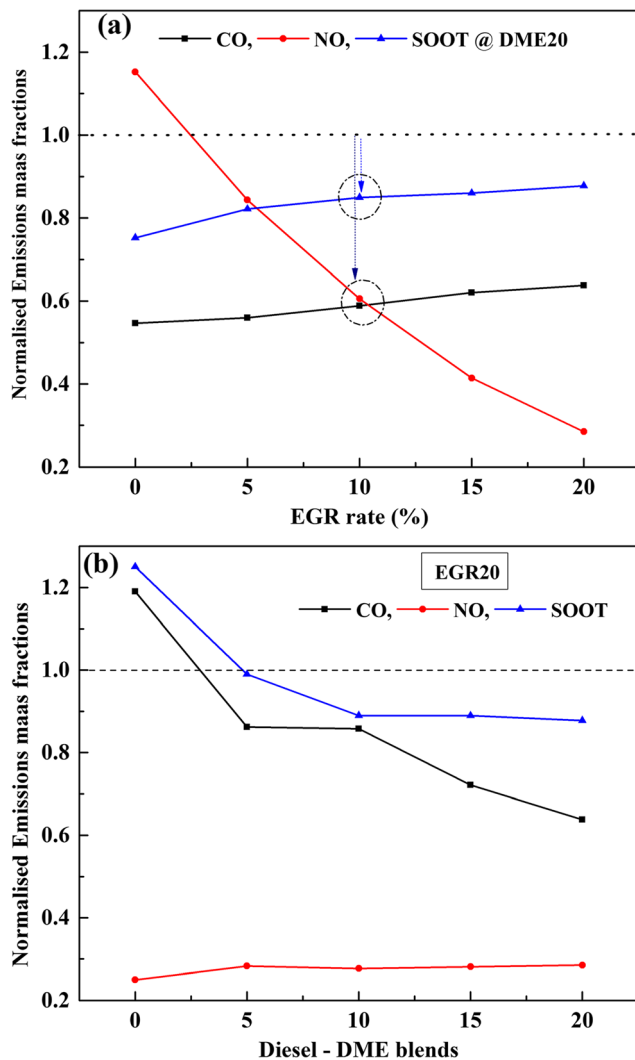**Fig. 8** Effects of DME/diesel blends ratio and EGR rate on soot mass fraction

Fig. 9 **a** Trade-off among exhaust emissions (NO, CO, soot) for DME20 at various EGR rate. **b** Trade-off among exhaust emissions (NO, CO, soot) for EGR 20 rate at various DME/diesel blends

performance, combustion, and exhaust emission characteristics of CRDI engine. The results are summarized as follows:

1. The cylinder pressure and temperature decrease as the DME/diesel blend ratio increases.
2. As EGR rate varies from 0 to 20%, the tail pipe NO emission decreases due to decrease in peak in-cylinder temperature.
3. In post-flame combustion, soot concentration increases marginally with an increase in EGR rate.
4. Compared to neat diesel, CO and soot formations are less for all the cases of DME/diesel blends.
5. Effect of EGR on CO and soot formations is less for all the cases of DME/diesel blends compared to neat diesel
6. Least soot formation is observed for DME20 blend without EGR rate and found to be decreased by 22% compared to neat diesel.

7. In the present range of study, maximum efficiency is obtained for DME20 compared to other blends including neat diesel. In other way, it can be said that high efficiency is obtained at higher DME/diesel blend ratio.
8. Trade-off among exhaust emissions (CO, NO, soot) and efficiency established the optimum operating condition, i.e., DME20 and EGR10.

References

Arcoumanis C, Bae C, Crookes R, Kinoshita E (2008) The potential of dimethyl ether (DME) as an alternative fuel for compression-ignition engines: a review. Fuel 87(7):1014–1030. doi:10.1016/j.fuel.2007.06.007

AVL Fire version (2011) ICE Physics & Chemistry, combustion, emission, spray. Wallfilm, AVL List GmbH

Basu A, Wainwright JM (2001) DME as a power generation fuel: performance in gas turbines. In Proceedings of the PETROTECH 2001 Conference, New Delhi, India.

Bo Z, Weibiao F, Jingsong G (2006) Study of fuel consumption when introducing DME or ethanol into diesel engine. Fuel 85(5):778–782

Cipolat D (2007) Analysis of energy release and NOx emissions of a CI engine fuelled on diesel and DME. Appl Therm Eng 27(11):2095–2103. doi:10.1016/j.applthermaleng.2006.11.016

Colin O, Benkenida A (2004) The 3-zones extended coherent flame model (ECFM3Z) for computing premixed/diffusion combustion. Oil Gas Sci Technol 59(6):593–609. doi:10.2516/ogst:2004043

Daly CA, Simmie JM, Würmel J, DjebaIli N, Paillard C (2001) Burning velocities of dimethyl ether and air. Combust Flame 125(4):1329–1340. doi:10.1016/S0010-2180(01)00249-8

Fattah IR, Kalam MA, Masjuki HH, Wakil MA (2014) Biodiesel production, characterization, engine performance, and emission characteristics of Malaysian Alexandrian laurel oil. RSC Adv 4(34):17787–17796. doi:10.1039/C3RA47954D

Han Z, Uludogan A, Hampson GJ, Reitz RD (1996) Mechanism of soot and NOx emission reduction using multiple-injection in a diesel engine, No. 960633, SAE Technical Paper.

Huang Z, Qiao X, Zhang W, Wu J, Zhang J (2009) Dimethyl ether as alternative fuel for CI engine and vehicle. Front Energy Power Eng Chin 3(1):99–108

Jeon J, Kwon SII, Park YH, Oh Y, Park S (2014) Visualizations of combustion and fuel/air mixture formation processes in a single cylinder engine fueled with DME. Appl Energy 113:294–301

Kajitani S, Oguma M, Mori T (2000) DME fuel blends for low-emission, direct-injection diesel engine. SAE Tech Paper No. 2000–01-2004. doi: 10.4271/2000-01-2004

Kapus PE, Cartellieri WP (1995) ULEV potential of a DI/TCI diesel passenger car engine operated on di-methyl ether SAE Paper. No. 952754. doi: 10.4271/952754

Kim MY, Yoon SH, Ryu BW, Lee CS (2008) Combustion and emission characteristics of DME as an alternative fuel for compression ignition engines with a high pressure injection system. Fuel 87(12):2779–2786. doi:10.1016/j.fuel.2008.01.032

Lee S, Seungmook O, Young C, Kernyong K (2011) Performance and emission characteristics of a CI engine operated with n-butane

blended DME fuel. Appl Therm Eng 31:1929–1935. doi:10.1016/j.applthermaleng.2011.02.039

Mobasheri R, Peng Z, Mirsalim SM (2012) Analysis the effect of advanced injection strategies on engine performance and pollutant emissions in a heavy duty DI-diesel engine by CFD modeling. Int J Heat Fluid Flow 33:59–69. doi:10.1016/j.ijheatfluidflow.2011.10.004

Park SH, Lee CS (2013) Combustion performance and emission reduction characteristics of automotive DME engine system. Prog Energy Combust Sci 39(1):147–168. doi:10.1016/j.pecs.2012.10.002

Rezgui Y, Guemini M (2014) Effect of ethanol addition on soot precursor's emissions during benzene oxidation in a jet-stirred reactor. Environ Sci Pollut Res 21(10):6671–6686. doi:10.1007/s11356-014-2582-8

Semelsberger TA, Borup RL, Greene HL (2006) Dimethyl ether (DME) as an alternative fuel. J Power Sources 156(2):497–511. doi:10.1016/j.jpowsour.2005.05.082

Sorenson SC (2001) Dimethyl ether in diesel engines: progress and perspectives. J Eng Gas Turbines Power 123(3):652–658. doi:10.1115/1.1370373

Suh HK, Lee CS (2008) Experimental and analytical study on the spray characteristics of dimethyl ether (DME) and diesel fuels within a common-rail injection system in a diesel engine. Fuel 87(6):925–932. doi:10.1016/j.fuel.2007.05.051

Teng H, McCandless JC, Schneyer JB (2004) Thermodynamic properties of dimethyl ether—an alternative fuel for compression-ignition engines. SAE Tech Pap Ser. No. 2004–01-0093. doi: 10.4271/2004-01-0093

Verbeek RP, Van DA, Van WM (1996) Global assessment of di-methyl ether as an automotive fuel. Second ed., 96.OR.VM.029.1/RV, TNO Road-Vehicles Research Institute.

Wang Y, Zhao Y, Yang Z (2013) Dimethyl ether energy ratio effects in a dimethyl ether-diesel dual fuel premixed charge compression ignition engine. Appl Therm Eng 54:481–487. doi:10.1016/j.applthermaleng.2013.02.005

Yao M, Zheng Z, Xu S, Fu M (2003) Experimental study on combustion process of dimethyl ether. SAE: 2003–01-3194. doi: 10.4271/2003-01-3194

Ying W, Longbao Z (2008) Experimental study on exhaust emissions from a multi-cylinder DME engine operating with EGR and oxidation catalyst. Appl Therm Eng 28:1589–1595. doi:10.1016/j.applthermaleng.2007.10.018

Zhu Z, Li DK, Liu J, Wei YJ, Liu SH (2012) Investigation on the regulated and unregulated emissions of a DME engine under different injection timing. Appl Therm Eng 35:9–14. doi:10.1016/j.applthermaleng.2011.08.015